

Fig. S1. Forskolin-induced endogenous IP₃R1 levels in a time-dependent manner. HEK-293 cells were treated with 10 μM forskolin for different time points (0, 3, 6, 9, 12 h). Western blotting revealed a time-dependent increase in the endogenous IP₃R1 protein levels upon forskolin treatment.

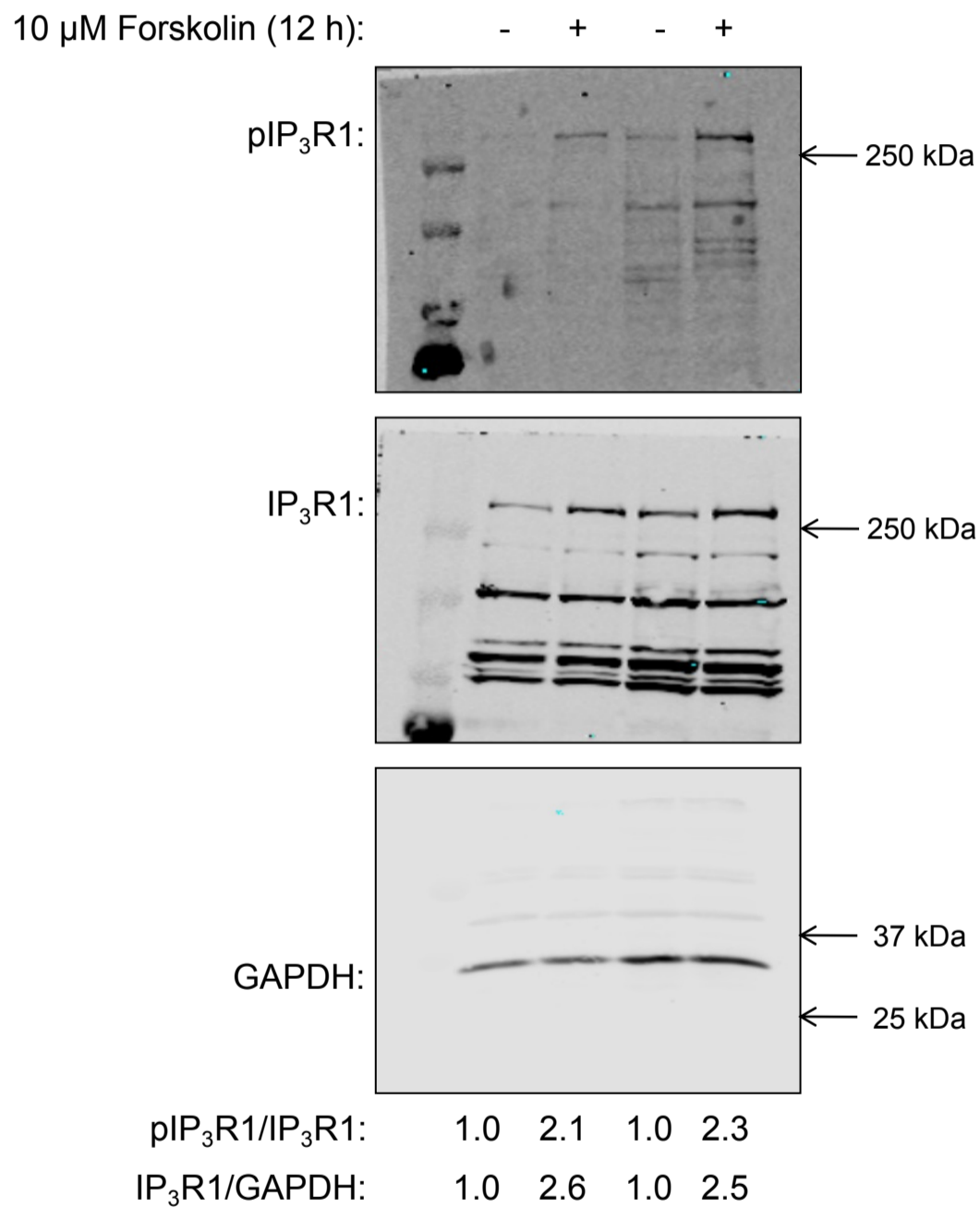


Fig. S2. Forskolin-induced phosphorylation of IP₃R1. HEK-293 cells were treated with 10 μ M forskolin for 12 hours. Western blots depicting increase in the phosphorylation of the endogenous IP₃R1 at the Ser-1756 residue and total IP₃R1 protein levels upon treatment with forskolin. (Lane numbers 1 & 2: 20 μ g protein and lane numbers 3 & 4: 30 μ g protein was loaded).

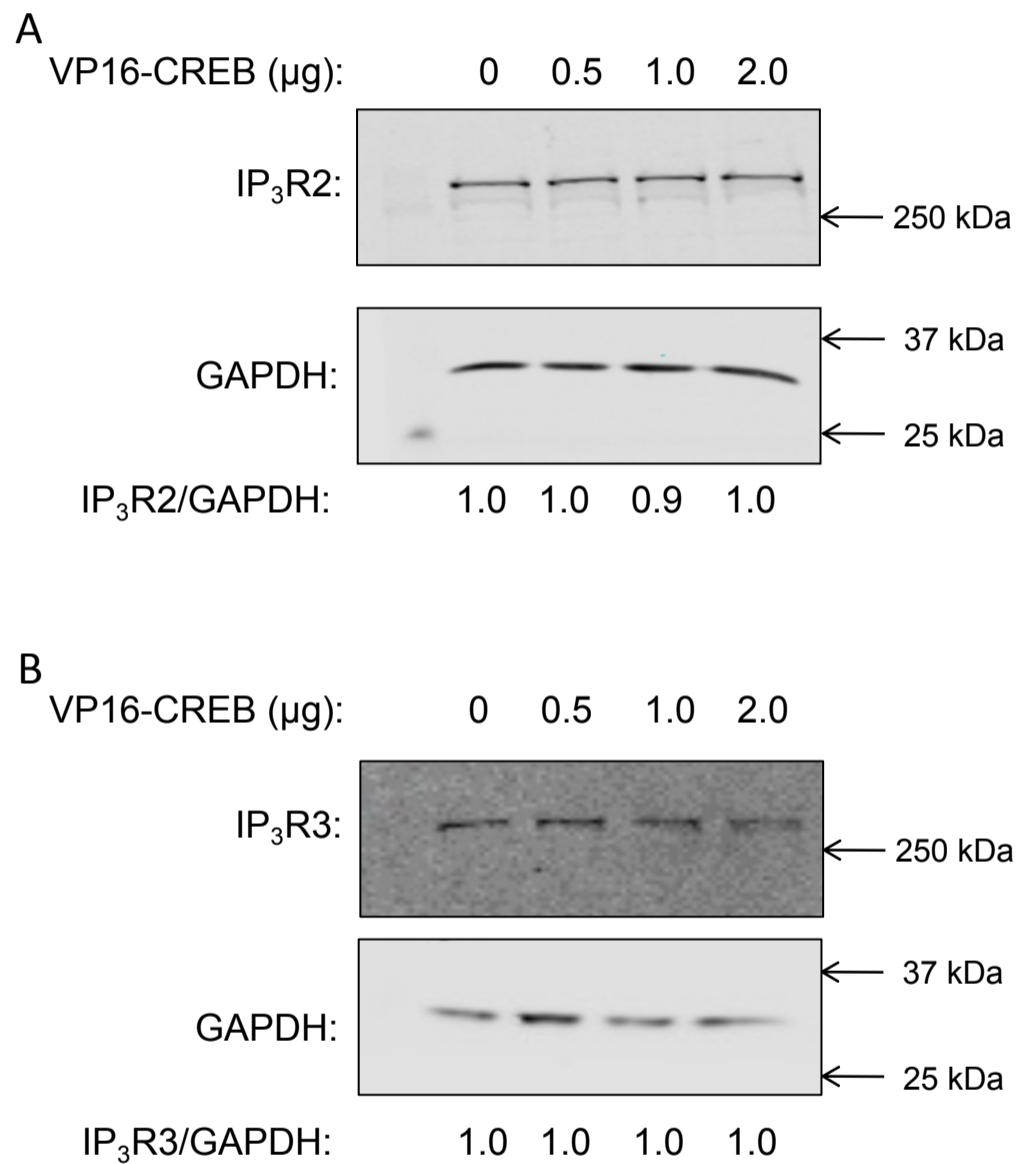


Fig. S3. CREB over-expression does not alter the endogenous protein levels of IP₃R2 and IP₃R3. HEK-293 cells were transiently transfected with increasing concentrations of VP16-CREB expression plasmid followed by Western blotting to determine the endogenous IP₃R2 and IP₃R3 protein levels using IP₃R2 and IP₃R3 specific antibodies. The endogenous (A) IP₃R2 and (B) IP₃R3 levels remained unchanged with increasing amounts of VP16-CREB expression plasmid.

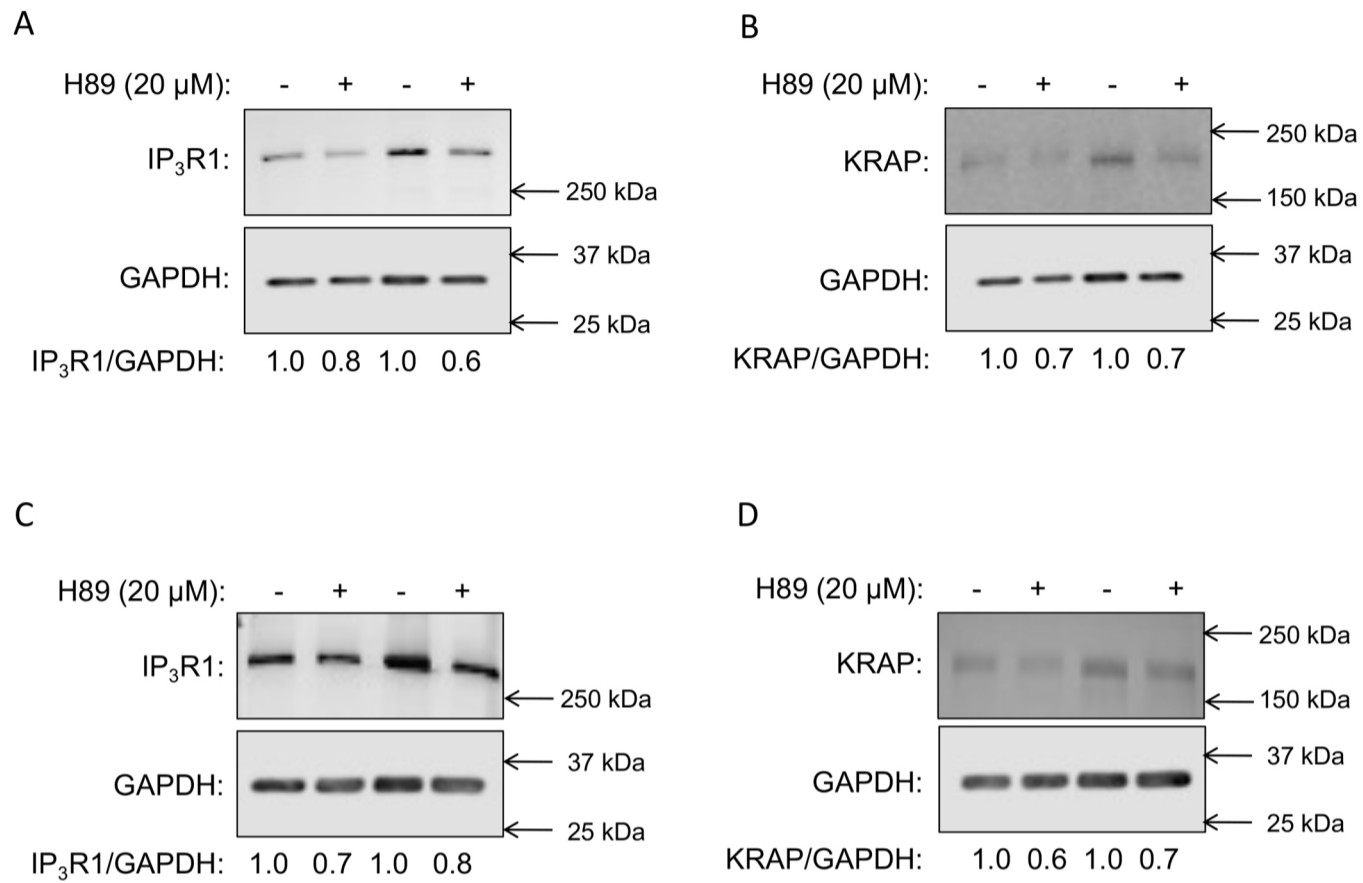


Fig. S4. H89 diminished the endogenous IP₃R1 and KRAP levels in SH-SY5Y and HeLa cells. SH-SY5Y and HeLa cells were treated with 20 μ M H89 for 12 hours followed by protein isolation and Western blotting. Western blots depicting decrease in the endogenous IP₃R1 and KRAP protein levels in (A, B) SH-SY5Y and (C, D) HeLa cells upon H89 treatment. (Lane numbers 1 & 2: 20 μ g protein and lane numbers 3 & 4: 30 μ g protein was loaded).

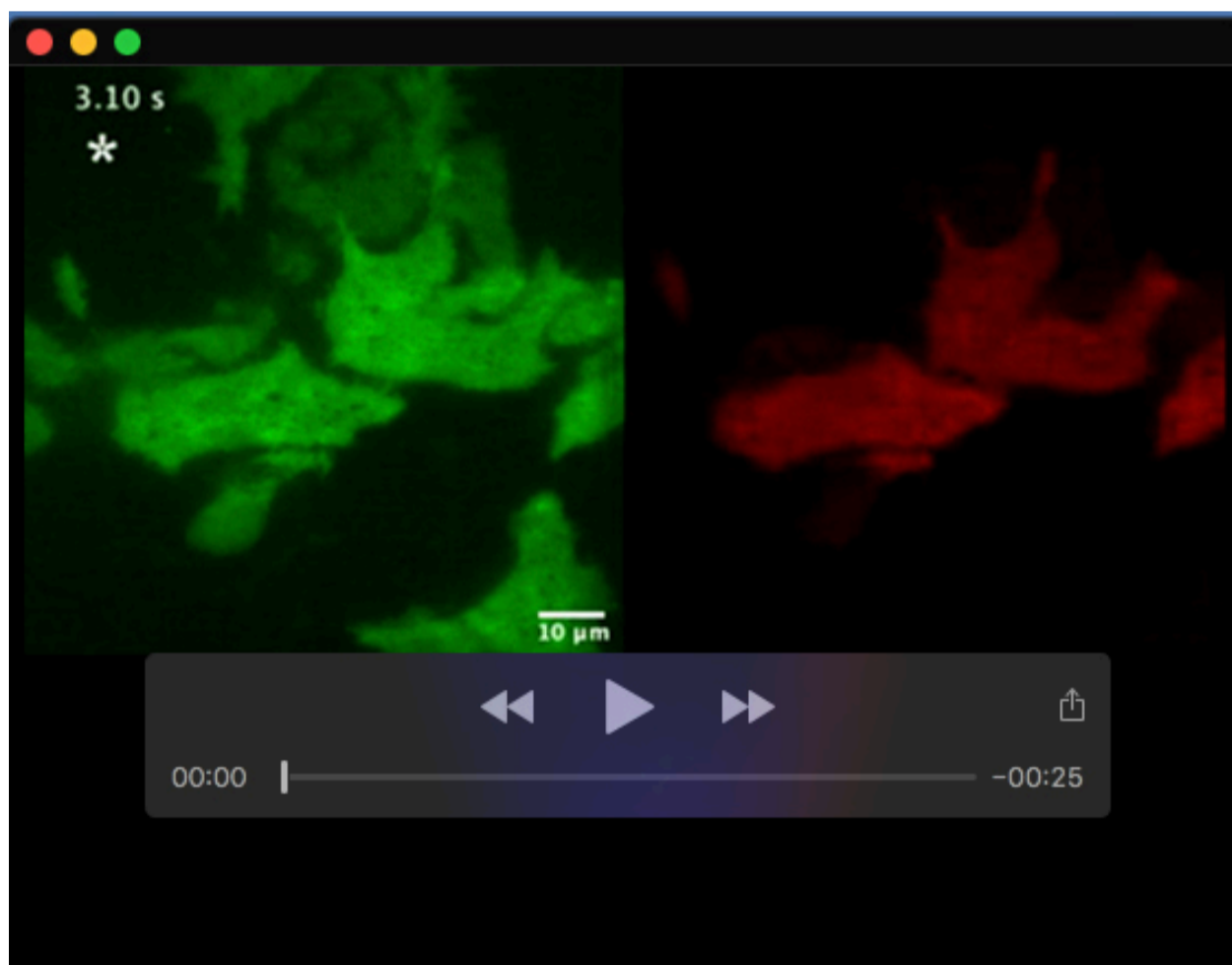
Table S1. Description of the nature of tissues, number of each tissue, TPMs for IP₃R1/2/3 and CREB.

No.	Tissue Sample	<i>CREB1</i> (TPM)	<i>ITPR1</i> (TPM)	<i>ITPR2</i> (TPM)	<i>ITPR3</i> (TPM)
1.	Adipose – Subcutaneous (n=663)	14.61	13.4	6.854	32.57
2.	Adipose - Visceral (Omentum) (n=541)	11.72	8.267	7.814	31.19
3.	Adrenal Gland (n=258)	5.899	11.95	15.59	18.4
4.	Artery – Aorta (n=432)	14.46	52.73	6.018	9.951
5.	Artery – Coronary (n=240)	13.45	59.83	7.48	23.03
6.	Artery - Tibial (n=663)	15.68	82.02	6.701	13.03
7.	Bladder (n=21)	12.9	28.67	5.517	25.74
8.	Brain – Amygdala (n=152)	4.015	4.2	4.464	2.842
9.	Brain - Anterior cingulate cortex (n=176)	4.413	21.54	4.466	3.338
10.	Brain - Caudate (basal ganglia) (n=246)	4.189	14.34	5.018	3.643
11.	Brain - Cerebellar Hemisphere (n=215)	14.01	19.74	2.093	5.415
12.	Brain – Cerebellum (n=241)	10.66	76.19	3.348	7.016
13.	Brain – Cortex (n=255)	4.516	34.52	5.34	5.491
14.	Brain - Frontal Cortex (n=209)	5.703	38.23	4.346	3.828
15.	Brain – Hippocampus (n=197)	4.214	5.737	2.987	3.149
16.	Brain – Hypothalamus (n=202)	4.89	4.515	3.337	4.013
17.	Brain - Nucleus accumbens (n=246)	4.264	13.04	4.522	3.837
18.	Brain - Putamen (n=205)	3.518	7.7	3.582	3.324
19.	Brain - Spinal cord (n=159)	7.121	2.611	6.579	7.828
20.	Brain - Substantia nigra (n=139)	4.345	4.135	3.588	4.662
21.	Breast - Mammary Tissue (n=459)	13.35	16.03	9.494	32.45
22.	Cells - Cultured fibroblasts (n=504)	15.21	4.17	5.777	46.68
23.	Cells - EBV-transformed lymphocytes (n=174)	20.64	25.17	29.77	35.6
24.	Cervix - Ectocervix (n=9)	18.18	18.34	7.894	37.12
25.	Cervix - Endocervix (n=10)	17.36	18.44	8.11	37.35
26.	Colon – Sigmoid (n=373)	11.02	24.68	10.78	23.53

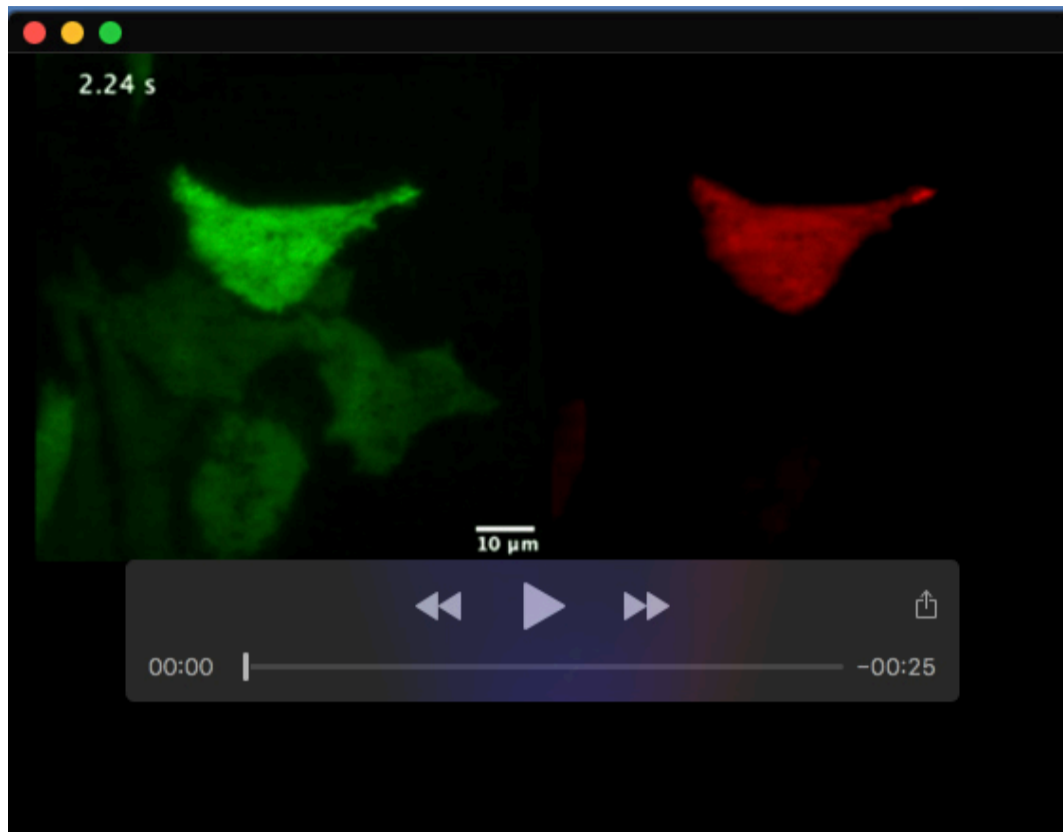
27.	Colon – Transverse (n=406)	8.59	11.21	5.755	43.48
28.	Esophagus - Gastroesophageal Junction (n=375)	9.977	40.34	5.519	24.22
29.	Esophagus – Mucosa (n=555)	9.181	5.766	10.06	31.55
30.	Esophagus - Muscularis (n=515)	9.75	41.08	6.212	22.67
31.	Fallopian Tube (n=9)	14.04	47.75	8.022	38.19
32.	Heart - Atrial Appendage (n=426)	4.623	6.396	3.523	11.35
33.	Heart - Left Ventricle (n=432)	3.437	3.212	1.535	8.767
34.	Kidney – Cortex (n=85)	3.749	7.076	4.516	12.99
35.	Kidney – Medulla (n=4)	6.812	11.92	5.666	27.96
36.	Liver (n=226)	2.865	1.304	8.559	1.829
37.	Lung (n=578)	13.63	20.26	7.498	72.36
38.	Minor Salivary Gland (n=162)	10.29	12.66	15.54	33.66
39.	Muscle – Skeletal (n=803)	3.132	1.61	1.39	3.889
40.	Nerve - Tibial (n=619)	15.74	12.7	8.456	135.8
41.	Ovary (n=180)	14.77	39.94	8.747	31.99
42.	Pancreas (n=328)	3.604	1.445	3.459	9.256
43.	Pituitary (n=283)	8.498	18.77	4.27	17.13
44.	Prostate (n=245)	11.26	20.87	5.242	33.15
45.	Skin - Not Sun Exposed (n=604)	11.32	3.817	13.62	107.1
46.	Skin - Sun Exposed (n=701)	11.21	5.94	14.71	105.5
47.	Small Intestine - Terminal Ileum (n=187)	10.8	13.55	6.769	64.36
48.	Spleen (n=241)	12.43	10.26	5.88	74.89
49.	Stomach (n=359)	6.33	6.782	4.091	36.49
50.	Testis (n=361)	17.57	6.888	3.91	44.57
51.	Thyroid (n=653)	13.48	34.69	6.175	133.3
52.	Uterus (n=142)	15.93	46.98	7.428	26.56
53.	Vagina (n=156)	13.84	12.97	8.965	56.42
54.	Whole Blood (n=755)	5.615	1.484	2.169	4.378

Table S2. *In silico* analysis revealed putative binding sites for CREB in the proximal promoter domains of KRAP gene.

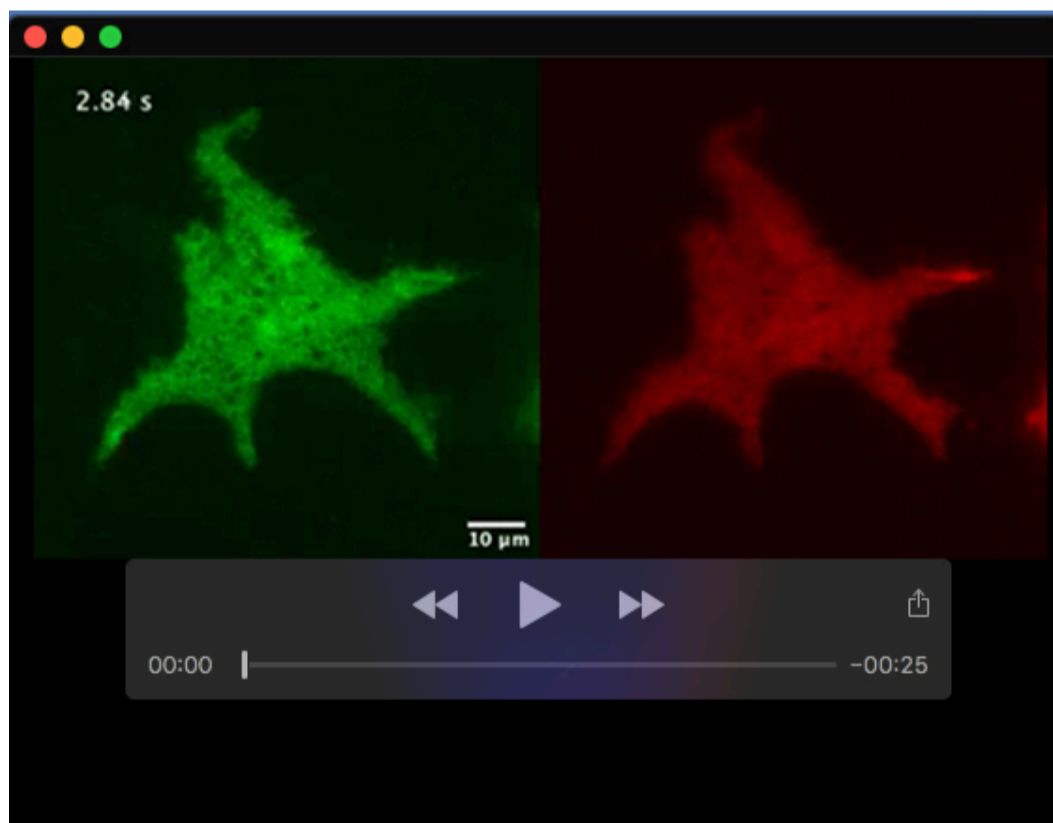
Tool	Alibaba2.1	TFBIND	ConSite	PROMO
	CREB	CREB	CREB	CREB
KRAP	-	+	+	-



Movie 1. A typical TIRF recording from hR1 endo cells co-transfected with pcDNA and mCherry plasmid. Video showing 3 s prior to photolysis of caged cilP₃ and the following 40 s of activity in Cal520-loaded hR1 endo cells, related to Fig. 7. Photolysis was accomplished by exposure from a 405 nm laser for 1 s (indicated by an asterisk). An image acquired from the same field of view using a 561 nm laser to optically identify mCherry positive cells is also shown.



Movie 2. A typical TIRF recording from hR1 endo cells co-transfected with KCREB and mCherry plasmid. Video showing 3 s prior to photolysis of caged cilP₃ and the following 40 s of activity in Cal520-loaded hR1 endo cells, related to Fig. 7. Photolysis was accomplished by exposure from a 405 nm laser for 1 s (indicated by an asterisk). An image acquired from the same field of view using a 561 nm laser to optically identify mCherry positive cells is also shown.



Movie 3. A typical TIRF recording from hR1 endo cells co-transfected with VP16-CREB and mCherry plasmid. Video showing 3 s prior to photolysis of caged cilP₃ and the following 40 s of activity in Cal520-loaded hR1 endo cells, related to Fig. 7. Photolysis was accomplished by exposure from a 405 nm laser for 1 s (indicated by an asterisk). An image acquired from the same field of view using a 561 nm laser to optically identify mCherry positive cells is also shown.